Express Polymer Letters Vol.18, No.10 (2024) 1051–1062
Available online at www.expresspolymlett.com
https://doi.org/10.3144/expresspolymlett.2024.80

Research article

Determination of the brittleness of glass fibers on selected mechanical and rheological properties of the polymer composite

Stanislav Miščík[1], *Jozef Dobránsky*[1*], *Miroslav Gombár*[2], *Robert Čep*[3]

[1]Technical University of Kosice, Faculty of Manufacturing Technologies with a seat in Presov, Sturova 31, 080 01 Presov, Slovakia
[2]University of West Bohemia Pilsen, Faculty of Mechanical Engineering, Univerzitní 8, 306 14, Plzeň, Czech Republic
[3]VSB – Technical University of Ostrava, Faculty of Mechanical Engineering, 17. listopadu 15, 708 00 Ostrava-Poruba, Czech Republic

Received 14 May 2024; accepted in revised form 18 July 2024

Abstract. The paper deals with the influence of the brittleness of glass fibers on the selected performance properties of the fibrous polymer composite. Understanding the fatigue behavior of fiber-reinforced plastics is desirable for exploiting their features in safe, durable, and reliable industrial components. Based on the proposed methodology, it is possible to assess the impact of material reuse on selected mechanical and rheological properties. To verify the methodology by experimental analysis, homopolymer PP reinforced with chemically grafted glass fiber (30 wt%) was selected. The proposed methodology was subsequently verified by experimental analysis and evaluated statistically. The morphology of the fracture surfaces was evaluated, and the fiber-polymer matrix adhesion was monitored at the interface of the fracture surfaces. Based on the measured and evaluated values and fracture surfaces, we can say that the brittleness of the fibers significantly affects the performance properties of the tested polymer composite.

Keywords: *polymer, composite, glass fiber, brittleness, mechanical properties*

1. Introduction

The article by Singh *et al*. [1] provides a rigorous review of the literature in the field of glass fiber composites. Fiberglass composite is a type of fiber reinforced polymer composites. Fiberglass composite has good properties such as low density, high strength and easy processing, so it is widely used in aerospace, automotive and construction industries.

Recently, more research has been conducted on glass fiber reinforced composites due to their excellent mechanical properties. Morampudi *et al.* [2] in their study dealt with the analysis of polymer composites reinforced with glass fibers made from different types of glasses prepared by different production technologies. As the volume of glass fibers increased, the properties of GFRP composites improved. The mechanical and thermal properties of various glass fiber reinforced polymer composites when subjected to mechanical loading have been studied and reported [2–4].

Recently, additional research has been conducted on glass fiber reinforced composites due to their excellent mechanical properties. As a new member of the silica derivative family, modified glass fiber (MGF) has attracted much attention for its excellent properties and potential applications. Surface treatment of glass fiber (GF) significantly changes its performance, leading to a series of changes in its surface

*Corresponding author, e-mail: jozef.dobransky@tuke.sk

structure, wettability, electrical properties, mechanical properties and stability [5–8].

The development of fracture mechanics test methods for the determination of delamination resistance or fracture toughness of fiber-reinforced, polymer-matrix composites is an active area of research. The emphasis in this review is on standardization of test methods. Recent developments leading towards new standardized test procedures will be presented, complementing and updating earlier reviews [9–11].

In addition to the positive effects on environmental sustainability, polymer recycling is also beneficial in terms of reducing production costs and material resources. The aim of the study by Jiun *et al.* [12] was to find out how the recycling cycle affects the physical properties and mechanical properties of the thermoplastic polymer and thermoplastic elastomer polymer. The obtained results showed that the tensile strength and density decreased for the thermoplastic polymer, and the appearance changes were significant when the number of recycling cycles increased [12–16].

Authors Mohammed *et al.* [17] in their study investigated the fracture behavior of a quasi-brittle material in the fracture processing zone. They performed a matrix of experimental work to investigate failure behavior based on a parameter known as the fragility number, which is a measure of brittle behavior. The results showed that the increase in the homogeneity of the composite laminates, which is introduced by inserting a certain angular layer for the laminate structure, increased the ductility of the material as the brittleness number increased. A larger sample size leads to an increase in brittleness for the same stacking sequences due to an increase in the stress concentration factor [17–21].

On the basis of the mentioned conclusions of the previous authors, research was proposed to determine the brittleness of glass fibers in a polymer composite. Mechanical and rheological properties were selected to assess the effect of brittleness of glass fibers. Understanding the fatigue behaviour of fibre-reinforced plastics is desirable for exploiting their features in safe, durable and reliable industrial components.

2. Experiment preparation

2.1. Materials

The test samples were manufactured from a composite known under the trademark Syntegum 1030 AFV. It is a composite of a homopolymer PP reinforced with chemically grafted glass fiber (30 wt%). It has been specially developed for hi tech parts operating at high temperatures and subject to considerable mechanical stresses. SYNTEGUM 1030 AFV 00 is characterized by a higher flexural modulus and a higher tensile strength at yield, thanks to the action of a grafting agent.

2.2. Preparation of material and test samples

Prior to experimental measurement, it was necessary to prepare material and test specimens. The preparation of the material took place simultaneously with the production of test specimens. The first batch of test specimens was made from virgin material. It was necessary to process enough material to be used for the production of further batches. The necessary part of the test samples from the thus produced batch (G1) is used for testing and the remaining material is scrapped. The scrap material was used for the second batch of material (G2). Again, the necessary part of the samples was used for testing and the remaining material was scrapped. This was the procedure until the production of the ninth batch (G9). Table 1 shows the designation of material batches.

From the prepared material (batch), multi-purpose Type A test bodies were injected for the purpose of the experimental analysis according to the standard EN ISO 3167, or, alternatively, 1A according to the standard EN ISO 527-2.

The injection process was carried out on a standard injection molding machine Demag Systec 100-310 according to technological parameters listed in the material sheet. After the end of the production cycle, the test pieces were conditioned at standard 23 °/50 *RH* conditions. Half of the test bodies used for simulation of the lifetime of the moldings depending on the recycled content were subjected to

Table 1. Designation of material batches.

Batch	Description
GV	Virgin material (without previous processing)
G1	Material after the first transition
G2	Material after the second transition
G3	Material after the third transition
G4	Material after the fourth transition
G5	Material after the fifth transition
G6	Material after the sixth transition
G7	Material after the seventh transition
G8	Material after the eighth transition
G9	Material after the ninth transition

an elevated temperature of 150 °C in a drier with forced-air circulation for 500 h prior to the study of their utility properties.

3. Methods

The experimental analysis took place in two stages. In the first, short-term performance properties were evaluated, where the tests were performed after conditioning the test specimens. In the second stage, the performance properties were evaluated by the method of exposing them to elevated temperature for a defined time, with an emphasis on product life.

3.1. Establishing rheological properties

The melt flow index (MFI) is a standardized technological test of thermoplastic materials that serves to evaluate the flow properties. The melt volume flow rate (*MVR*) was chosen for testing. The *MVR* was determined by a thermo Haake meltflow MT rheometer according to the EN ISO 1133 standard with conditions 230 °C and load 2.16 kg.

3.2. Establishing tensile properties

The test is conducted under the specified pretreatment conditions, ambient and speed parameters of the test bodies defined by EN ISO 527-1/2. The test bodies were stretched in the direction of their main longitudinal axis until disrupted, at a constant speed of 5 mm/min. During the test, the values of the applied load and the increase in the initially measured length of the test piece were recorded. 10 test bodies from each batch were tested on the Tiratest 2300 tearing machine. The test body was placed and fastened to the jaws of the tearing machine so that the longitudinal axis of the body was identical to the axis of the machine and so that release of the test piece would be prevented. The module of tensile elasticity was determined at a reduced test speed 1 mm/min, measured by Epsilon – model 3542-010M-025-ST strain gauge (Figure 1).

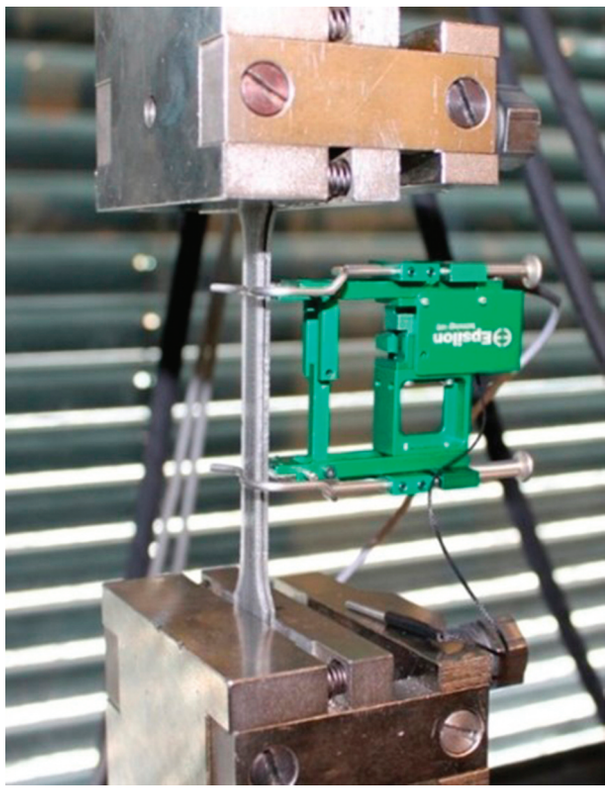

Figure 1. Placement the strain gauge on the test sample on the Tiratest 2300.

3.3. Microscopic analysis of fracture areas of composites after the tensile test

Samples for observation of SEM images were sputtered with carbon to improve the conductivity of the sample. The samples were subsequently observed on a TESCAN MIRA 3 FE electron microscope with an integrated EDX analyzer from Oxford Instruments, which allows observation of the microstructure of the material and the performance of elemental analysis (spot, surface distribution). For SEM images, the secondary electron mode (SE) and an accelerating voltage of 10 kV were used. The distance between sample and detector was 18 mm and view field 185 μm. All captured SEM images were taken from the surface fractured sections located at the central parts of the testing articles as obtained during uniaxial tensile testing.

3.4. Evaluation of fiber brittleness

Samples of individual batches were fired in a laboratory furnace at a temperature of 600 °C, where the polymer matrix and glass fibers were separated. Subsequently, the separated glass fibers were transferred to a microscope slide and measured under an optical microscope with a digital camera. Subsequently, the results were evaluated in Excel. Measurements were repeated twice for each batch of material.

4. Results and discussion

4.1. Evaluation of fiber brittleness

As can be seen from Figure 2, fiber length, as a parameter characterizing the fragility of the investigated parameter, is significantly ($p < 0.000$) influenced by the number of transitions, remelting of the material (batch of material) in the sense of Fisher's

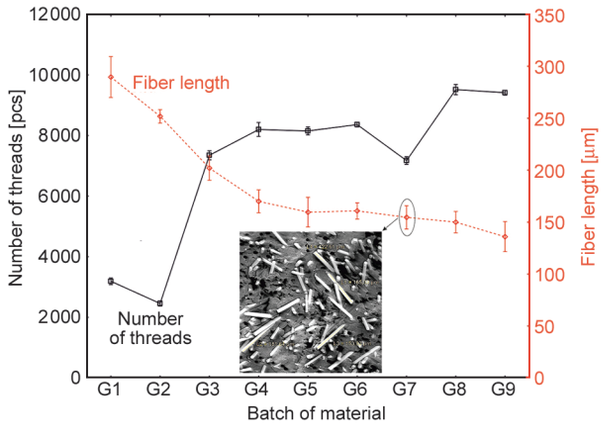

Figure 2. Effect of the number of material transitions (batch) on the length of glass fibers in the composite.

analysis of variance (ANOVA). It is obvious that by increasing the number of reflows of the material, the average fiber length gradually decreases. Here it is necessary to say that the second analyzed variable in Figure 3, namely the number of threads, so this data is only informative and we will not consider it further in the study, due to the nature of this variable. This behavior agreed with data observed by authors Al-Oqla and Sapuan [22] and Pessey *et al.* [23].

The basic monitored variable, within Figure 2, is the average length of the fibers in the material. The average increase in the number of fibers represents 194.955% between the G1 transition and the G9 transition.

The second observed quantity in Figure 2 is the average length of the fibers in the material. Here it is possible to observe a gradual decrease in the length of the fibers with an increasing number of material transitions. After the first transition (G1), the average length of the fibers is at the level of 289±19.7 µm. After the second transition (G2), the length of the fibers in the material decreases to 251±6.5 µm, which represents a decrease of 14.149%. In order, the third transition (G3) brings the average fiber length at the level of 202±11.7 µm, while the inter-transition decrease in fiber length represents 19.522% (49±9.1 µm). After the fourth transition (G4), we observe the average fiber length at the level of 170±11.1 µm, which represents a decrease compared to the G3 transition by 15.842% (32±11.4 µm). After the fifth transition (G5), the rate of decrease in the average fiber length compared to the G4 transition decreases and reaches the level of 6.471%, while after the fifth transition the average fiber length is at the level of 159±14.3 µm. A slight increase in the average fiber length occurs after the sixth transition (G6), while the change compared to the G5 transition represents only –0.629% in relative terms. The seventh transition (G7) causes a further decrease in the average fiber length to the level of 154±11.2 µm, while the decrease in relative terms represents 3.750%. After the eighth transition (G8), the decrease in the average length decreases again compared to the G7 transition in relative terms by 2.597%, while the average value after the G8 transition is 150±10.3 µm last transition, the average length of the fibers in the material is at the level of 136±14.4 µm, which represents a decrease of 9.333%. The change in the average fiber length from the first realized transition (G1) to the last realized transition (G9) represents 52.941%, which represents an average decrease of 6.618% per one transition. The results also confirm the conclusion of Ng *et al.* [24], Kim and Choi [25] and Varga and Bartha [26].

4.2. Evaluation of rheological properties

In this case, the basic dependently evaluated transformation is the melt volume flow rate (*MVR*), the change of which is analyzed depending on the number of material transitions. The examined dependence is shown in Figure 3.

It is clear from Figure 3 that by increasing the number of material transitions, the *MVR* value increases. In the case of virgin material (GV), which was the input to the experiment (without previous processing of the material), the *MVR* value is at the level of 4.000±0.708 cm^3/10 min. From the point of view of ANOVA, the batch of material represents a significant

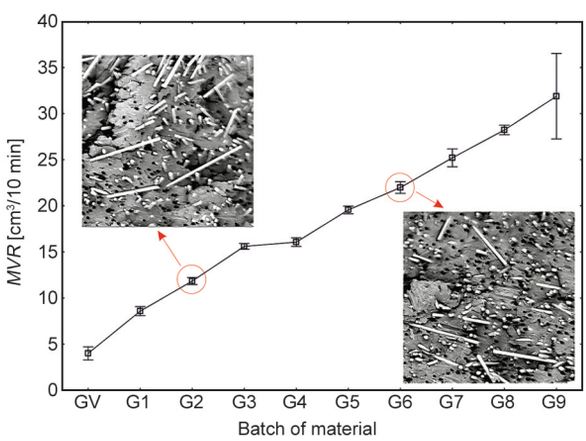

Figure 3. The effect of the number of material transitions (batch) on the *MVR*.

influence that affects the changes in the *MVR* value ($p < 0.000$) at the chosen significance level $\alpha = 5\%$ with 98.220% influence.

After the first transition (G1), the value of the investigated variable increases to the value of 8.580±0.492 cm^3/10 min, while this increase represents a difference at the level of 4.580±3.245 cm^3/10 min (114.5%) and at the same time the difference is significant ($p < 0.001$) at the selected level of significance $\alpha = 0.05$. After the second transition (G2), the value of the investigated variable (*MVR*) increases to a value of 11.840±0.379 cm^3/10 min, while the increase in the value of *MVR* compared to the previous batch (G1) represents 37.995% (3.260±2.663 cm^3/10 min), while also this difference between the *MVR* value of transition G2 and transition G1 is statistically significant ($p = 0.007$). After the implementation of the third transition (G3), the *MVR* value is at the level of 15.600±0.317 cm^3/10 min, which represents an increase of 3.760±2.663 cm^3/10 min (31.757%; $p < 0.001$). A change in the increase in *MVR* occurs at the fourth transition (G4). Here there will be an increase in the value of the investigated variable to the level of 16.060±0.470 cm^3/10 min, while the *MVR* difference between the fourth (G4) and third (G3) transitions is 0.460 cm^3/10 min (2.949%), while this difference is not significant ($p = 1.000$). During further transitions (G5 to G9), the conditional *MVR* value gradually increases (Figure 3) from a value of 19.560±0.417 cm^3/10 min at G5 to a value of 31.880±4.630 cm^3/10 min after the last transition (G9). Although the *MVR* value with the number of transitions (G1 to G9) increases with the average level of change of the *MVR* value per transition at the level of 3.098 cm^3/10 min, this increase decreases in relative terms from 114.500% after the first transition (G1) to 12.970% after last transition (G9). The results also confirm the conclusion of Zhang *et al.* [27] and Huang *et al.* [28].

4.3. Evaluation of tensile properties

In this case, the basic values evaluated are the Tensile strength σ_m [MPa], the tensile strain at strength ε_m [%] and the tensile modulus E_t [MPa]. The variable input variables are the batch of material, which expresses the number of transitions and the condition of the material (before aging and after aging). In the following text, we will evaluate the individual evaluated quantities separately.

4.3.1. Evaluation of tensile strength

The first evaluated value is the tensile strength σ_m [MPa]. A graphic representation of the effect of the number of transitions on the tensile strength for the material before and after aging is shown in Figure 4. The average value of σ_m for both material states and all considered batches of material is 55.354±3.044 MPa. The number of transitions is the most significant influence with 96.910% influence on the change in the value of σ_m, while this influence is statistically significant ($p < 0.000$) at the chosen level of significance $\alpha = 0.05$. The influence of the material condition on the change in the value of σ_m represents only 2.620% ($p < 0.000$). However, for both states of the material, the value of σ_m decreases by increasing the number of transitions, and at the same time, in the entire range of transitions, the value of σ_m for the material before aging is higher than for the material after aging.

The starting value of σ_m for the material before aging after the first transition (G1) is 89.043±1.421 MPa. After the next transition (G2), the value of σ_m decreases to the level of 75.445±0.665 MPa, which represents a decrease of 13.598±1.101 MPa (15.601%). At the same time, the difference in the value of σ_m between the transition G1 and G2 is significant ($p < 0.000$) at the chosen level of significance $\alpha = 0.05$. After the third transition (G3), the value of σ_m drops to 65.019±0.442 MPa, which represents a decrease compared to the second transition (G2) by 10.426±1.101 MPa (13.831%). The difference in the value of σ_m between the second and third transition is also statistically significant ($p < 0.000$). The intermediate rate of decline thus decreases from the value

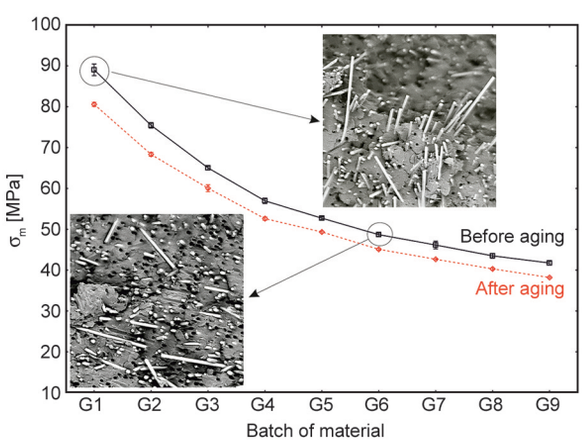

Figure 4. The effect of the number of material transitions (batch) on the σ_m for material before aging and material after aging.

of 15.601% (G1–G2) to the value of 13.831% (G2–G3). The fourth transition causes a further decrease in the value of σ_m to an average value of 56.963±0.653 MPa. The decrease compared to the third transition (G3) thus represents 8.056±0.101 MPa (12.390%, $p < 0.000$). After the fifth transition of the material (G5), the value of σ_m decreases to a value of 52.714±0.350 MPa, while the intermediate drop (G5–G4) of σ_m represents 7.459% (4.249 MPa; $p < 0.000$). After the next transition (G6), the value of σ_m decreases again to the value of 48.679±0.406 MPa with the value of the inter-transition decrease at the level of 4.035 MPa (7.654%; $p < 0.000$). As shown in Figure 2, the value of σ_m also decreases after the seventh transition (G7) to a value of 46.140±0.934 MPa, after the eighth transition (G8) to a value of 43.493±0.590 MPa and also after the last, ninth transition (G9) to its final value 41.754±0.450 MPa. However, the rate of inter-transition decrease decreases from a value of 2.539 MPa (5.216%) between G7–G6 to a value of 1.739 MPa (3.998%) between transitions G9–G8.

Based on Figure 4, a similar trend can also be seen in the material after aging, where after the first transition (G1) the value of σ_m is at the level of 80.580±0.500 MPa and at the same time after the last transition (G9) at the level of 38.180±0.184 MPa. If we compare the total change in the value of σ_m between the first and last transition, before and after aging, then for the material before aging, this difference in tensile strength is 47.289 MPa (53.108%), and for the material after aging, the difference σ_m is at the level of 42.400 MPa (52.619%). On average, 5.911 MPa (6.639%) for material before aging and 5.300 MPa (6.577%) for material after aging per transition (batch of material). The average difference between the value of σ_m between both states of the material is 4.681±0.511 MPa, with a gradually decreasing value of the difference in the average values of σ_m for individual transitions (batch of material) from the value of 8.463±0.960 MPa (G1), through 7.105±0.571 MPa (G2), 4.979±0.652 MPa (G3), 4.363±0.532 MPa (G4) up to a value of 3.574±0.317 MPa after the last material transition (G9).

Based on the previous analyses, it is possible to derive certain relationships between the studied characteristics, (σ_m), the fiber length and (*MVR*), focusing on the tensile strength σ_m. Dependencies are graphically displayed in Figure 5. The relationship between σ_m and fiber length is shown in Figure 5a. From the figure, it follows that with the increasing number of transitions, the values of σ_m and fiber length decrease. A more detailed analysis of individual monitored variables is presented above. The mutual relationship between the σ_m and the length of the fibers expressed by the correlation index reaches the value of 0.9710 ($p < 0.0000$), that is, according to Cohen's scale of the definition of the absolute value of the correlation coefficient, the analyzed relationship represents a functional dependence. Since the third variable, which is the number of transitions is also included in the analysis, the partial correlation with consideration of the i nfluence of the batch of material between the variables of σ_m and fiber length reaches a value of 0.8879 ($p < 0.0000$). At the same time, the relationship between the batch of material and the σ_m reaches the value –0.9440 ($p < 0.0000$) and between the batch of material and the length of the fibers the value –0.8829 ($p < 0.0000$).

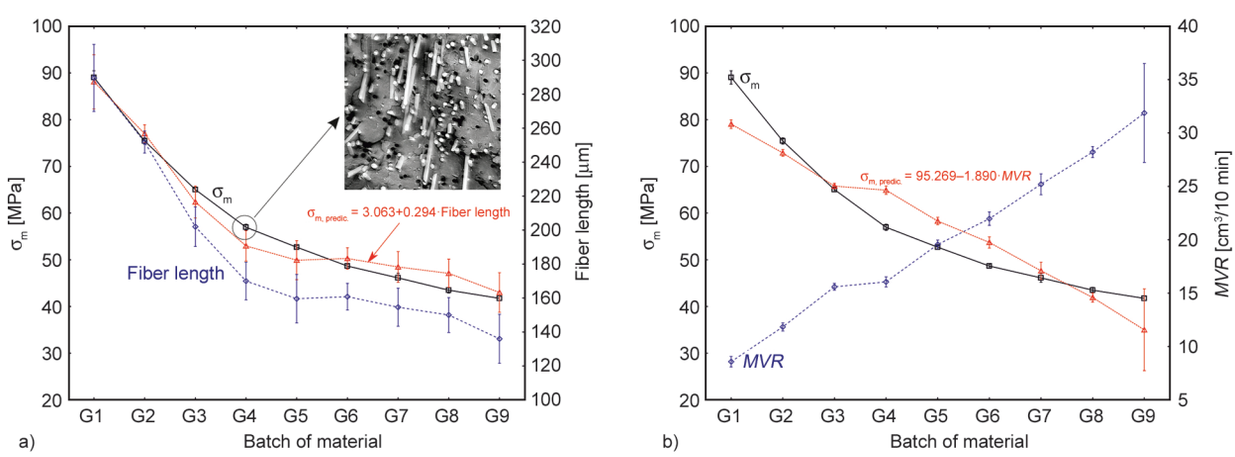

Figure 5. Change in σ_m, fiber length (a) and *MVR* (b) for individual batches of material (material before aging).

It is also possible to identify a mutual link between the σ_m and the *MVR* (Figure 5b). Based on the correlation index, it is possible to identify a functional relationship between the two investigated variables (σ_m, *MVR*) with a correlation coefficient value of –0.9184 ($p < 0.0000$). At the same time, it is possible to identify a negative bond, *i.e.* increasing the value of *MVR* conditionally decreases the value of σ_m. However, the influence of the batch of material on the relationship between σ_m and *MVR* makes the relationship between the investigated variables not significant ($p = 0.3220$) and reaches the level of 0.1498. At the same time, however, the relationship between the batch of material and *MVR* reaches a value of 0.9827 ($p < 0.0000$). This behavior agreed with data observed by authors Chen *et al.* [29], Valášek *et al.* [30] and Manas *et al.* [31].

4.3.2. Evaluation of tensile strain strength

The tensile strain at strength (ε_m) as the second monitored tensile property depending on the number of transitions for the material before and after aging is shown in Figure 6. Within the basic analysis, the most significant variable that affects the change in the ε_m value is the material condition, with 84.860% influence on its change, while the material condition is a significant factor ($p < 0.0000$) at the chosen significance level $\alpha = 5\%$. The number of transitions affects the change in the value of ε_m by 10.450% ($p < 0.0000$), and the mutual interaction of the condition and the batch of material has only a 4.120% effect on the change in the value of the investigated response ε_m ($p < 0.0000$).

In terms of the mentioned dependence (Figure 6), it is clear that the change in the value of ε_m for the material before aging and after aging is significantly different. In the state of the material before aging after the first transition (G1), the value of ε_m is at the level of 3.583±0.169%. After the second transition (G2), the value of ε_m drops to the level of 3.114±0.169%, which represents an inter-relative transition decrease of the value of ε_m by 13.090%. The difference in value between G2 and G1 (0.469%) is significant ($p < 0.000$) at the selected level of significance $\alpha = 5\%$. After the third transition (G3), the value of ε_m is 2.740±0.065%, which represents a relative decrease compared to the G2 transition by 12.010% ($p < 0.000$). After the fourth transition (G4), the value of ε_m was reached at the level of 2.478±0.041%. The inter-transition decrease

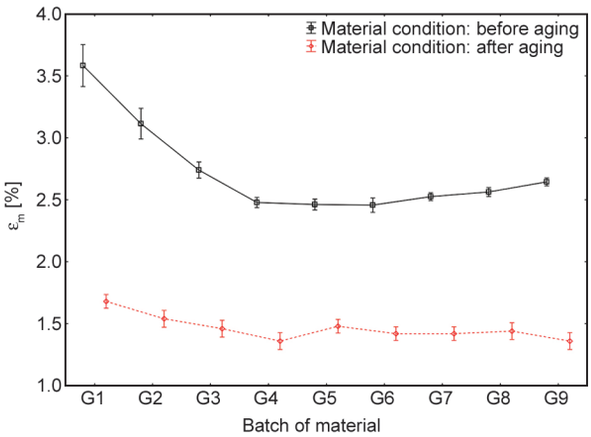

Figure 6. The effect of the number of material transitions (batch) on the ε_m for the material before aging and the material after aging.

represents 9.562% ($p < 0.000$). In order, the fifth transition of the material (G5) brings another but significantly more moderate decrease in the value of ε_m to the level of 2.462±0.044%, and this decrease in relative terms represents 0.646% ($p = 1.000$). After the sixth transition (G6), the value of ε_m slightly decreases to the level of 2.457±0.058% (0.203%, $p < 0.000$) and with the seventh transition (G7) to the value of 2.526±0.031%, which represents an inter-transition increase of 2.808% ($p = 0.912$). A further increase in the value of ε_m is also observed during the last two transitions of the material, to a value of 2.563±0.036% (1.465%, $p = 1.000$) after the eighth transitions (G8) and to a value of 2.645±0.032% (3.199%, $p = 0.731$) after the ninth transition (G9).

The average value of ε_m for the state of the material after aging is 1.462±0.032%. After the first transition (G1), the value of ε_m is at the level of 1.680±0.056%. After the second transition (G2) in the sense of Figure 6, the value of ε_m drops to the level of 1.540±0.068%, which represents a relative inter-transition decrease of 8.333%. The resulting difference in the value of ε_m between the first (G1) and the second transition (G2) thus represents 0.140%, while this difference is statistically significant ($p = 0.029$) at the chosen level of significance $\alpha = 0.05$. After the next, third transition (G3), there will be a further decrease in the value of ε_m to the level of 1.460±0.068%, which represents a relative decrease of 5.159% (0.080%, $p = 0.763$) with the previous transition. After the fourth transition (G4), the value of ε_m decreases to the level of 1.360±0.068%, which at the same time represents the minimum value of the investigated response ε_m for the material after

aging. The inter-transition decrease in relative terms is 6.849% (0.100%, $p = 0.388$). After the fifth transition (G5), there will be a slight increase in the ε_m value to the level of 1.480±0.068%, which at the same time represents an increase of 8.824% in relative terms compared to the G4 transition (0.120, $p = 0.127$). The sixth (G6) and seventh (G7) transitions yield the same value of ε_m at the level of 1.420±0.068%, which represents a decrease of 4.054% compared to the fifth transition (G5). A slight increase to a value of 1.440±0.068% is observed after the eighth transition (G8) with a subsequent decrease to a value of 1.360±0.068% after the last transition (G9). The difference in proportional elongation between the first (G1) and the last (G9) transition is 0.320%, which in relative terms is 19.048%. If we observe the difference between the ε_m value between the material before and after aging, the average deviation between both states of the material is 1.267±0.068%. The maximum difference is observed in the batch of material G1 with a value of 1.903% ($p < 0.000$) and, on the other hand, the minimum difference in the batch of material G5 with a value of 0.982% ($p < 0.000$).

Based on the performed analysis, it is possible to draw the conclusion that, in addition to the fact that the change in the value of ε_m is influenced by the batch of material and the condition of the material, we also observe the connection of ε_m with the average length of the fibers (Figure 7a). The correlation between ε_m and the average fiber length given by the correlation coefficient reaches a value of 0.908 ($p < 0.000$). If we also consider the influence of the batch of material in this connection, the value of the partial correlation coefficient will reach the value of 0.875 ($p < 0.000$), which represents a very significant degree of mutual connection. At the same time, the correlation coefficient between the ε_m and the batch of material reaches the value –0.693 ($p < 0.000$) and between the batch of material and the average length of the fibers the value –0.883 ($p < 0.000$).

The analysis of the relationship between the investigated response and the value of ε_m and the number of fibers (Figure 7a) shows the fact that the value of the correlation coefficient reaches the value –0.841 ($p < 0.000$), which represents a very significant relationship, and at the same time, as the number of fibers in the material increases, the value decreases ε_m.

The relationship between ε_m and *MVR* (Figure 7b) expressed by the correlation coefficient reaches the value of –0.658 ($p < 0.000$), however, when considering the batch of material as a third moderating variable, this relationship was not confirmed as significant ($p = 0.279$) and the partial correlation coefficient reaches the value of 0.167. This behavior agreed with data observed by authors Zhang *et al.* [32] and Berube *et al.* [33].

4.3.3. Evaluation of tensile modulus

The third monitored variable is the tensile modulus E_t [MPa]. The total average value of E_t for all samples is 6644.567±191.074 MPa, while the average value of E_t for the material before aging is 6799.933±290.397 MPa and for the material after aging is 6489.200±251.318 MPa. However, for both states of the material, the value of E_t decreases by increasing the number of transitions (Figure 8). The influence of the number of transitions on the change

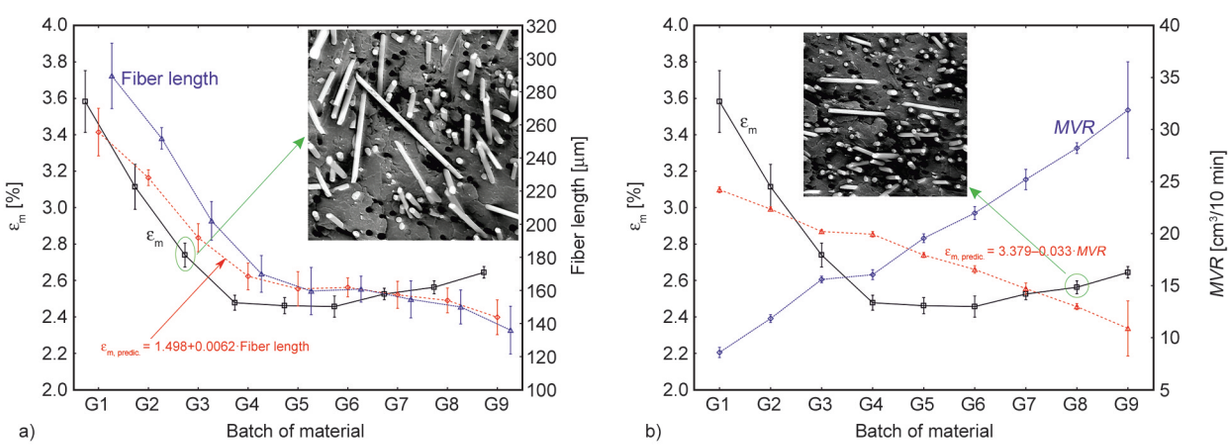

Figure 7. Change in the value of the ε_m, the fiber length (a) and the *MVR* (b) for individual batches of material (material before aging).

in the value of E_t is 95.660% and the batch of material is a significant predictor ($p < 0.000$) at the chosen level of significance $\alpha = 5\%$. The condition of the material is a statistically significant predictor ($p < 0.000$), but with only a 2.930% influence on the change in E_t value. In the end, the interaction of the batch of material and the state of the material is also a significant predictor ($p < 0.000$), but its influence on the change in the value of E_t reaches only 0.860%.

The starting value of E_t after the first transition of the material (G1) before aging is 8389±146.311 MPa. After the second transition (G2), the value of E_t drops to the level of 7853.4±44.298 MPa, which represents an intermediate decrease of 535.6±95.305 MPa, which in relative terms represents a decrease of 6.385%. The difference in E_t values between transition G1 and G2 is significant ($p < 0.000$) at the $\alpha = 0.05$ significance level. After the third transition (G3), the value of E_t decreases to the level of 7492.4±36.122 MPa with an inter-transition difference in absolute terms of 361±40.210 MPa (4.597%, $p < 0.000$). After the fourth transition (G4) again, according to Figure 8, the value of E_t decreases to the level of 7245±105.350 MPa. The intermediate decrease thus represents 246.8±70.736 MPa, which in relative terms represents 3.294% ($p < 0.000$). After the fifth transition (G5), the E_t value reaches the level of 6763.6±65.288 MPa. The difference in average values of E_t between transition G4 and G5 reaches 480±85.319 MPa (6.652%, $p < 0.000$). After the sixth transition (G6), Et reaches a value of 6253±51.029 MPa, which represents a decrease compared to transition G5 by 510.6±58.159 MPa (7.549%, $p < 0.000$). The decrease at the level of 3.305% (189.8±59.925 MPa) occurs after the seventh transition (G7) when the value of E_t reaches 6063.2±62.820 MPa. The last significant decrease in E_t is observed between transition G7 and G8 (5641.2±70.717 MPa) by 6.960% (422±66.769 MPa, $p < 0.000$) followed by a slight decrease in the value of E_t after transition G9 (5498±46.184 MPa) by 2.528% ($p = 0.221$). The difference between the first (G1) and the last transition (G9) thus represents 2891 MPa, which makes an average of 361.375 MPa per pass.

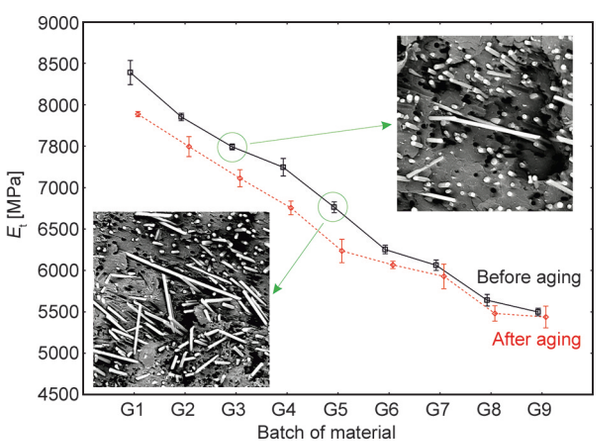

Figure 8. The effect of the number of material transitions (batch) on the E_t for the material before aging and the material after aging.

For the material after aging, the starting value of E_t after the first transition (G1) is at the level of 7887.2±30.609 MPa, and the change of this value with the batch of material copies the change of the E_t value of the material before aging. The difference in E_t value between the material before aging and after aging is 310.733±31.658 MPa. In the sense of Figure 9 it is clear that the biggest difference in the value of E_t between the investigated material states is observed in the batch of material G5, namely 527.6 MPa ($p < 0.000$). The second largest difference is observed in the value of E_t for batch G1, namely 501.8 MPa ($p < 0.000$). The differences in E_t values between the material before and after aging from material batch G7 are no longer statistically significant ($p = 0.321$ (G7), $p = 0.097$ (G8), 0.998 (G9)) and thus the E_t values before and after aging in the mentioned material batches can be considered the same.

The mutual relationship between E_t and the average length of fibers in the material before aging (Figure 9a) reaches the level of a very significant relationship based on the value of the correlation coefficient (0.889, $p < 0.000$). When the average fiber length decreases, the average E_t value also decreases. However, if we also consider the influence of the batch of material as a moderating variable, then the mutual relationship between E_t and the length of the fibers was not proven based on the partial correlation coefficient (0.231, $p = 131$). At the same time, however, there is a significant relationship between the batch of material and the value of E_t at the level of –0.993 ($p < 0.000$). Figure 10 also shows the prediction ($E_{t,\,predict}$) of the value of E_t, while the average deviation between the model and the actual value of E_t is -0.484% with a minimum negative value of the deviation at the level of –13.8% and a maximum positive value of the deviation at the level of 12.7%.

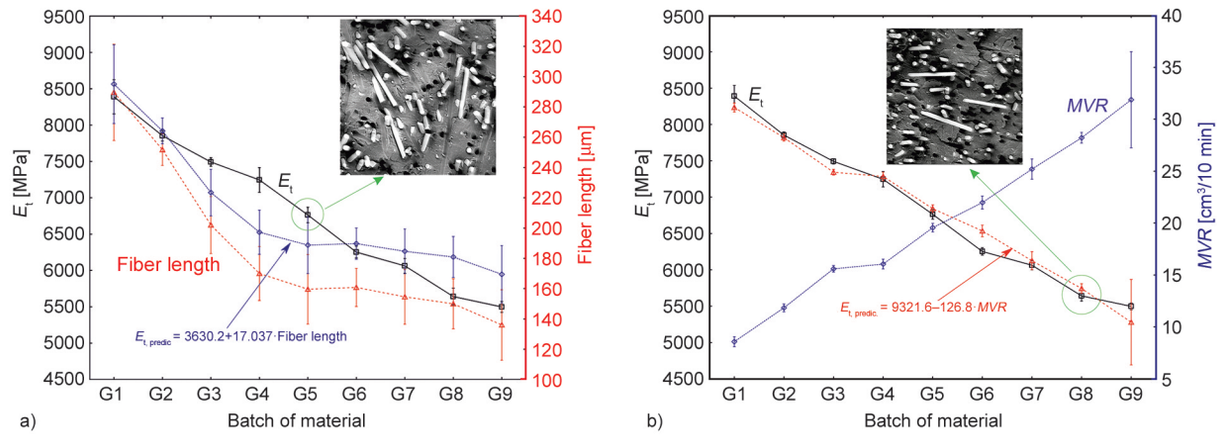

Figure 9. Change in the value of the E_t, the fiber length (a) and *MVR* (b) for individual batches of material (material before aging).

Figure 9b represent the analysis of the relationship between E_t and *MVR*.

The correlation between the value of E_t and *MVR* (Figure 9b) expressed by the correlation coefficient reaches the value –0.973 ($p < 0.000$). When increasing the value of the average number of fibers, the value of E_t decreases simultaneously. However, if we also consider the influence of the batch of material, then the correlation between the studied variables (E_t, *MVR*) reaches a value of 0.106, but the partial correlation coefficient is not statistically significant ($p = 0.492$).

The relationship between the impact strength (A_c) and the brittleness of the investigated material, expressed as the length of the glass train, is shown in Figure 10. As it is obvious, with gradual remelting of the material (G1 to G9) the average fiber length decreases and in accordance with this decrease, the conditional value of the impact strength of the investigated material also decreases. If in the first step we focus on the relationship between the two described properties depending on the remelting of the material, then the value of the Pearson correlation coefficient between the impact strength and the remelting of the material (batch of material) reaches the value –0.904 ($p < 0.000$) and between the brittleness of the material (fiber length) and material remelting (material batch) value –0.883 ($p < 0.000$). This behavior agreed with data observed by authors Espinach *et al.* [34] and Branciforti *et al.* [35].

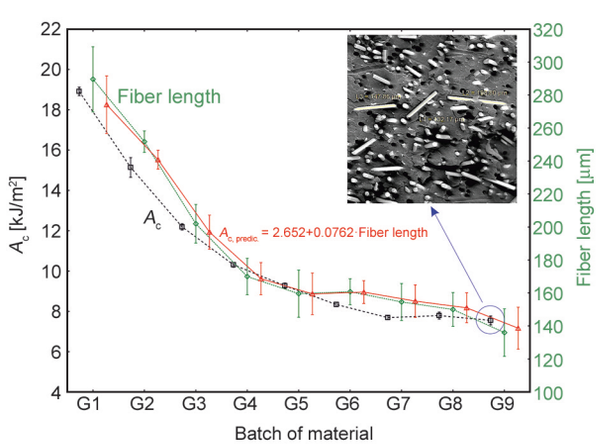

Figure 10. Relationship between impact strength and brittleness (fiber length) of the examined material depending on the degree of remelting (batch of material).

The mutual relationship, expressed by the correlation coefficient, between the impact strength (A_c) and the brittleness of the examined material is 0.968 ($p < 0.000$). This value points to a very significant relationship between the studied variables, and by reducing the value of the impact strength, the fragility of the fibers also decreases, as shown in Figure 10. However, if we also consider the influence of remelting of the material (batch of material), the value of the partial correlation coefficient reaches the value of 0.846 ($p < 0.000$).

5. Conclusions

Based on the evaluated results of the mechanical and rheological properties of the composite, the theory about the influence of fiber length on the user properties of the material was confirmed. In the achieved results, we can observe a perfect correlation between the length of the fibers and the user properties of the material. With the successive number of transitions of the material through the injection machine and the mold, the rheological properties increased. The opposite trend was noted for mechanical properties, where the mechanical properties decreased with the

number of transitions. This result was also confirmed by analyzes of the fracture surfaces of the material. When testing samples exposed to elevated temperature, the differences in the measured results were minimal. In further research, the authors will focus on the analysis of the influence of fiber brittleness on other useful properties of this polymer composite.

Acknowledgements

This research has been elaborated in the framework of the projects VEGA no. 1/0488/23 and VEGA no. 1/091/22 were granted by the Ministry of Education, Science, Research and Sport of the Slovak Republic and this publication is the result of the Project implementation: Development of excellent research capacities in the field of additive technologies for the Industry of the 21st century, ITMS: 313011BWN5, supported by the Operational Program Integrated Infrastructure funded by the ERDF.

References

[1] Singh J., Kumar M., Kumar S., Mohapatra S. K.: Properties of glass-fiber hybrid composites: A review. Polymer-Plastics Technology and Engineering, **56**, 455–469 (2017). https://doi.org/10.1080/03602559.2016.1233271

[2] Morampudi P., Namala K. K., Gajjela Y. K., Barath M., Prudhvi G.: Review on glass fiber reinforced polymer composites. Materials Today-Proceedings, **43**, 314–319 (2021). https://doi.org/10.1016/j.matpr.2020.11.669

[3] Aiello M. A., Focacci F., Nanni A.: Effects of thermal loads on concrete cover of fiber-reinforced polymer reinforced elements: Theoretical and experimental analysis. ACI Materials Journal, **98**, 332–339 (2001).

[4] El-Assal A. M., Khashaba U. A.: Fatigue analysis of unidirectional GFRP composites under combined bending and torsional loads. Composite Structures, **79**, 599–605 (2007). https://doi.org/10.1016/j.compstruct.2006.02.026

[5] Wu Y., Song Y., Wu D., Mao X., Yang X., Jiang S., Zhang C., Guo R.: Recent progress in modifications, properties, and practical applications of glass fiber. Molecules, **28**, 2466 (2023). https://doi.org/10.3390/molecules28062466

[6] Nugroho G., Budiyantoro C.: Optimization of fiber factors on flexural properties for carbon fiber reinforced polypropylene. Journal of Composites Science, **6**, 160 (2022). https://doi.org/10.3390/jcs6060160

[7] Kugler S. K., Kech A., Cruz C., Osswald T.: Fiber orientation predictions – A review of existing models. Journal of Composites Science, **4**, 69 (2020). https://doi.org/10.3390/jcs4020069

[8] Hirano N., Muramatsu H., Inoue T.: Study of fiber length and fiber-matrix adhesion in carbon-fiber-reinforced polypropylenes. Advanced Composite Materials, **23**, 151–161 (2014). https://doi.org/10.1080/09243046.2013.844891

[9] Brunner A. J., Blackman B. R. K., Davies P.: A status report on delamination resistance testing of polymer-matrix composites. Engineering Fracture Mechanics, **75**, 2779–2794 (2008). https://doi.org/10.1016/j.engfracmech.2007.03.012

[10] Budzik M. K., Wolfahrt M., Reis P., Kozlowski M., Sena-Cruz J., Papadakis L., Saleh M. N., Machalicka K. V., de Freitas S. T., Vassilopoulos A. P.: Testing mechanical performance of adhesively bonded composite joints in engineering applications: An overview. Journal of Adhesion, **98**, 2133–2209 (2022). https://doi.org/10.1080/00218464.2021.1953479

[11] Safaei S., Akhavan-Safar A., Jalalvand M., da Silva L. F. M.: A new technique to measure shear fracture toughness of adhesives using tensile load. International Journal of Solids and Structures, **262**, 112091 (2023). https://doi.org/10.1016/j.ijsolstr.2022.112091

[12] Jiun Y. L., Tze C. T., Moosa U., Tawawneh M. A.: Effects of recycling cycle on used thermoplastic polymer and thermoplastic elastomer polymer. Polymers and Polymer Composites, **24**, 735–739 (2016). https://doi.org/10.1177/096739111602400909

[13] Liu F., Li T., Xu F., Li J., Jiang S.: Microstructure, tensile property, and surface quality of glass fiber-reinforced polypropylene parts molded by rapid heat cycle molding. Advances in Polymer Technology, **2020**, 3161068 (2020). https://doi.org/10.1155/2020/3161068

[14] Grigore M. E.: Methods of recycling, properties and applications of recycled thermoplastic polymers. Recycling, **2**, 24 (2017). https://doi.org/10.3390/recycling2040024

[15] Sikora J. W.: Special issue: Processing, structure, dynamics and mechanical properties of polymeric materials. Materials, **15**, 3143 (2022). https://doi.org/10.3390/ma15093143

[16] Gaspar-Cunha A., Covas J. A., Sikora J.: Optimization of polymer processing: A review (Part II-Molding technologies). Materials, **15**, 1138 (2022). https://doi.org/10.3390/ma15031138

[17] Mohammed Y., Hassan M. K., Abu El-Ainin H., Hashem A. M.: Effect of stacking sequence and geometric scaling on the brittleness number of glass fiber composite laminate with stress raiser. Science and Engineering of Composite Materials, **21**, 281–288 (2014). https://doi.org/10.1515/secm-2013-0038

[18] Abdellah M. Y., Hassan M. K., AlMalki A. A., Mohamed A. F., Backar A. H.: Finite element modelling of wear behaviors of composite laminated structure. Lubricants, **10**, 317 (2022). https://doi.org/10.3390/lubricants10110317

[19] Swolfs Y., Geboes Y., Gorbatikh L., Pinho S. T.: The importance of translaminar fracture toughness for the penetration impact behaviour of woven carbon/glass hybrid composites. Composites Part A: Applied Science and Manufacturing, **103**, 1–8 (2017). https://doi.org/10.1016/j.compositesa.2017.09.009

[20] Monticeli F. M., Fuga F. R., Donadon M. V.: A systematic review on translaminar fracture damage propagation in fiber-reinforced polymer composites. Thin-Walled Structures, **187**, 110742 (2023). https://doi.org/10.1016/j.tws.2023.110742

[21] Carvelli V., Lomov S. V., Sapozhnikov S. B., Breite C., Swolfs Y.: Fatigue of hybrid fibre-reinforced plastics. Philosophical Transactions of the Royal Society A: Mathematical Physical and Engineering Sciences, **381**, 20210222 (2023). https://doi.org/10.1098/rsta.2021.0222

[22] Al-Oqla F. M., Sapuan S. M.: Natural fiber reinforced polymer composites in industrial applications: Feasibility of date palm fibers for sustainable automotive industry. Journal of Cleaner Production, **66**, 347–354 (2014). https://doi.org/10.1016/j.jclepro.2013.10.050

[23] Pessey D., Bahlouli N., Pattofatto S., Ahzi S.: Polymer composites for the automotive industry: Characterisation of the recycling effect on the strain rate sensitivity. International Journal of Crashworthiness, **13**, 411–424 (2008). https://doi.org/10.1080/13588260802030745

[24] Ng H. Y., Lu X. H., Lau S. K.: Thermal conductivity, electrical resistivity, mechanical, and rheological properties of thermoplastic composites filled with boron nitride and carbon fiber. Polymer Composites, **26**, 66–73 (2005). https://doi.org/10.1002/pc.20076

[25] Kim K-S., Choi N-S.: Effects of thermal shock fatigue on short glass fiber-reinforced PBT composites embedded by thermally conductive particles. Journal of Mechanical Science and Technology, **29**, 4665–4670 (2015). https://doi.org/10.1007/s12206-015-1012-2

[26] Varga C., Bartha L.: Improving mechanical properties of glass fibre reinforced PBT waste for its recycling as a product of pipe system elements. Polymers and Polymer Composites, **24**, 609–616 (2016). https://doi.org/10.1177/096739111602400807

[27] Zhang S., Tan L., Liang J., Huang H., Jiang G.: Relationship between structure and properties of reprocessed glass fiber reinforced flame retardant poly(butylene terephthalate). Polymer Degradation and Stability, **105**, 140–149 (2014). https://doi.org/10.1016/j.polymdegradstab.2014.04.009

[28] Huang J., Lu X., Zhang G., Qu J.: Study on the rheological, thermal and mechanical properties of thermoplastic polyurethane/poly(butylene terephthalate) blends. Polymer Testing, **36**, 69–74 (2014). https://doi.org/10.1016/j.polymertesting.2014.03.006

[29] Chen L., Luo Y., Hu Z., Lin G-P., Zhao B., Wang Y-Z.: An efficient halogen-free flame retardant for glass-fibre-reinforced poly(butylene terephthalate). Polymer Degradation Stability, **97**, 158–165 (2012). https://doi.org/10.1016/j.polymdegradstab.2011.11.003

[30] Valášek P., Ruggiero A., Müller M.: Experimental description of strength and tribological characteristic of EFB oil palm fibres/epoxy composites with technologically undemanding preparation. Composites Part B: Engineering, **122**, 79–88 (2017). https://doi.org/10.1016/j.compositesb.2017.04.014

[31] Manas D., Manas M., Gajzlerova L., Ovsik M., Kratky P., Senkerik V., Skrobak A., Danek M., Manas M.: Effect of low doses beta irradiation on micromechanical properties of surface layer of injection molded polypropylene composite. Radiation Physics and Chemistry, **114**, 25–30 (2015). https://doi.org/10.1016/j.radphyschem.2015.04.022

[32] Zhang D., He M., Qin S., Yu J., Guo J., Xu G.: Study on dynamic mechanical, thermal, and mechanical properties of long glass fiber reinforced thermoplastic polyurethane/poly(butylene terephthalate) composites. Polymer Composites, **39**, 63–72 (2018). https://doi.org/10.1002/pc.23902

[33] Berube K. A., Lopez-Anido R. A., Goupee A. J.: Determining the flexural and shear moduli of fiber-reinforced polymer composites using three-dimensional digital image correlation. Experimental Techniques, **40**, 1263–1273 (2016). https://doi.org/10.1007/s40799-016-0127-4

[34] Espinach F. X., Julian F., Verdaguer N., Torres L., Pelach M. A., Vilaseca F., Mutje P.: Analysis of tensile and flexural modulus in hemp strands/polypropylene composites. Composites Part B: Engineering, **47**, 399–343 (2013). https://doi.org/10.1016/j.compositesb.2012.11.021

[35] Branciforti M. C., Oliveira C. A., de Sousa J. A.: Molecular orientation, crystallinity, and flexural modulus correlations in injection molded polypropylene/talc composites. Polymers for Advanced Technologies, **21**, 322–330 (2010). https://doi.org/10.1002/pat.1431